JACS
JOURNAL OF THE AMERICAN CHEMICAL SOCIETY

ARTICLE

pubs.acs.org/JACS

Continuous Flow Enzyme-Catalyzed Polymerization in a Microreactor

Santanu Kundu,[†,#] Atul S. Bhangale,[‡,#] William E. Wallace,[†] Kathleen M. Flynn,[†] Charles M. Guttman,[†] Richard A. Gross,[*,‡] and Kathryn L. Beers[*,†]

[†]Polymers Division, National Institute of Standards and Technology, Gaithersburg, Maryland 20899, United States

[‡]Polytechnic Institute of NYU, Brooklyn, New York 11201, United States

Supporting Information

ABSTRACT: Enzymes immobilized on solid supports are increasingly used for greener, more sustainable chemical transformation processes. Here, we used microreactors to study enzyme-catalyzed ring-opening polymerization of ε-caprolactone to polycaprolactone. A novel microreactor design enabled us to perform these heterogeneous reactions in continuous mode, in organic media, and at elevated temperatures. Using microreactors, we achieved faster polymerization and higher molecular mass compared to using batch reactors. While this study focused on polymerization reactions, it is evident that similar microreactor based platforms can readily be extended to other enzyme-based systems, for example, high-throughput screening of new enzymes and to precision measurements of new processes where continuous flow mode is preferred. This is the first reported demonstration of a solid supported enzyme-catalyzed polymerization reaction in continuous mode.

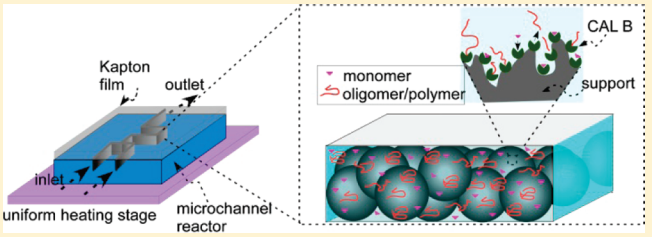

INTRODUCTION

Industrial biotechnology uses genetically engineered whole cells (e.g., bacteria, yeasts), plants, and isolated enzymes in chemical manufacturing processes. The basic tool set available to develop bioprocesses continues to rapidly grow providing exciting new opportunities to develop products such as biobased monomers, polymers, and biofuels.[1−3] Such growth is fueled by government incentives and a social push toward sustainable development. However, catalyst efficiency and process engineering challenges remain to develop cost-effective products. One bioprocess opportunity is the use of isolated enzymes (*in vitro* catalysis) to replace toxic metal catalysts enabling more benign process conditions for a wide range of chemical transformations.[4] Particularly, enzymes immobilized on solid supports have been used to synthesize biodegradable polyesters at lower temperatures and without many precautions (e.g., exclusion of moisture and oxygen) required for conventional catalysts; however, these polymerization reactions, similar to many processes that involve a biological entity, are complex relative to conventional manufacturing routes.[5−8] Complexities associated with any polymerization reaction, such as change in transport properties as the viscosity of the system increases with the progress of polymerizations, are further compounded by: (1) participation of bound water on enzymes in reactions as initiators and regulators of enzyme activity,[5,6] (2) the nonmonotonic change of enzyme activity with temperature,[5,9,10] and (3) the stability of adsorbed enzymes on solid supports.[11] In this paper, we aim to investigate these complex systems by precisely controlling the experimental parameters using a novel microchannel reactor or microreactor in continuous flow mode. Our results provide critical insight into these processes and will establish a framework for the development and characterization of continuous flow polymerization reactions using solid-supported enzymes.

Conducting polymerization reactions in microreactors offers several advantages over traditional batch synthesis methods, such as improved temperature control, low waste generation, and safer experimental conditions.[12,13] In addition, reactor design/configuration and reaction parameters can be varied easily and systematically. Furthermore, processes can be scaled up from laboratory scale to industrial scale. In the past, we successfully performed atom transfer radical polymerizations[14] and anionic polymerizations in microreactors.[15] Here, microreactors were used to study solid supported (immobilized) enzyme-catalyzed ring-opening polymerization (ROP) of lactones in continuous flow conditions. We took advantage of (1) high catalyst surface area to the reactor volume and (2) improved transport properties in the microreactors. The model reaction we chose is the ROP of ε-caprolactone (ε-CL) to polycaprolactone (PCL), using immobilized *Candida antartica* Lipase B (CAL B) in the form of Novozym 435 (N435), a widely used commercial biocatalyst.[5,6,10] Although enzymes have been used in microreactors previously, very few studies reported the use of solid supported enzymes to study organic synthesis or polymerization reactions.[16] This is likely due to the difficulty in loading of immobilized enzyme beads in microreactors and the high pressure drop across the microchannel because of increasing viscosity of polymer products. By implementing a suitable reactor design and performing reactions in semidilute organic

Received: January 5, 2011
Published: March 25, 2011

dx.doi.org/10.1021/ja111346c | *J. Am. Chem. Soc.* 2011, 133, 6006–6011

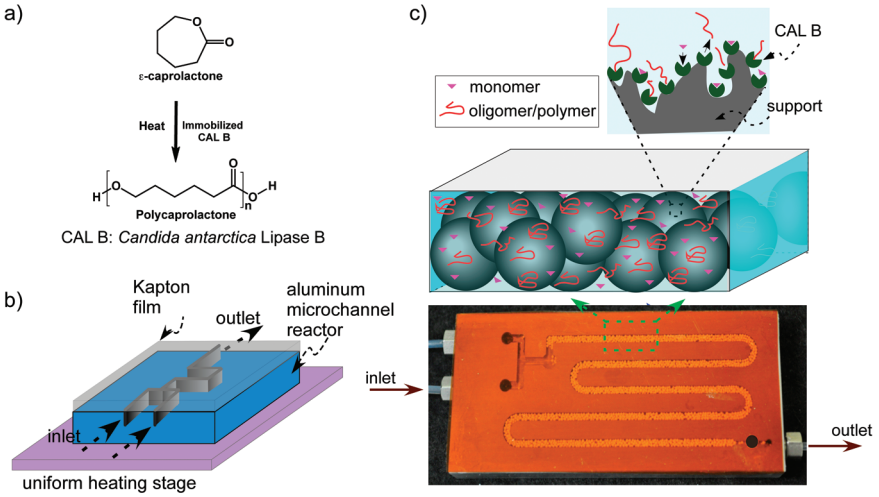

Figure 1. (a) Reaction scheme for ring-opening polymerization of ε-caprolactone to polycaprolactone. (b) Schematic of the microreactor setup. The microreactor was made of aluminum and was covered with Kapton film using a thermally cured epoxy. The microreactor was placed on a uniform heating stage for temperature control. (c) Image shows photograph of a typical microreactor used in this study. CAL B immobilized solid beads (macroporous polymethyl methacrylate) were filled in the channel. Polymerization reactions took place at enzyme active sites. The residence time for the reactants inside microreactors was changed by varying the flow rate.

media, we have overcome these problems and achieved (1) faster polymerization rates and (2) higher PCL molecular masses compared to that obtained in batch reactors at similar experimental conditions.

EXPERIMENTAL SECTION

Chemicals. All chemicals used were obtained from Sigma Aldrich, Inc. Novozym N435, a commercially available immobilized lipase preparation with *Candida antarctica* Lipase B (CAL B) physically immobilized on mesoporous polymethylmethacrylate supports (Lewatit VP OC 1600), was obtained from Novozymes. The molecular mass of CAL B is 33 000 g/mol. Typically, the amount of CAL B present in N435 beads is 10% by mass based on supplier specifications. Amount of CAL B on N435 was further confirmed by elemental analysis for nitrogen content. To control the amount of CAL B used in microreactor experiments, N435 beads were sieved to obtain a narrow bead size distribution (400 ± 50 μm). Since water is an initiator, care was taken to dry and to store the reactants and N435 beads. Sieved N435 beads were preserved over desiccants in a vacuum desiccator. ε-CL and toluene were dried over anhydrous calcium hydride and 4 Å activated molecular sieves. Water content of toluene, ε-CL, and N435 beads, measured using a Metrohm Coulometric Karl Fischer titrator, was 0.003, 0.025, and 0.46% by mass, respectively. Thus, the major source of water in reactions is N435 beads.

Batch Reactors. ε-CL ROP batch reactions were performed in 25 mL round-bottom flasks sealed with a rubber septum and maintained under an argon environment. Reaction flasks were placed in a heated oil bath with a feedback temperature controller. Using a syringe, 2 mL of dry toluene was introduced in the flask containing 100 mg of N435. After toluene reached the experimental temperature, 1 mL of ε-CL was added in the flask. Here, the mass ratio of CAL B to ε-CL was maintained at 1:100. Using a magnetic stirrer, the reaction mixture was stirred at 60 rad/s. Reaction temperature was monitored by inserting a thermocouple in the mixture. Samples were collected at different time intervals, using a syringe, to determine %-conversion and PCL molecular mass. All experiments were performed at least three times to determine the experimental variability. Control experiments were performed using beads without enzyme (Lewatit VP OC 1600) at the highest experimental temperature of 100 °C and no significant conversion was observed.

Microreactor Platform. Microchannels with dimensions of 2 mm, 1 mm, and 260 mm in width (W), depth (D), and length (L), respectively, were milled on a 10 mm thick aluminum block. Microchannel cross section was selected in order to facilitate the loading of beads. The channels were covered with Kapton film using ResinLab epoxy adhesive (E950g) and the epoxy was treated at 120 °C to obtain sufficient adhesive strength. The channels were filled with 100 mg of N435 beads of diameter 400 ± 50 μm by applying vacuum at one end of the reactor and introducing beads at the other end. The packing fraction (ε) of the beads was estimated as ≈0.5 by flowing toluene through the reactor. Considering a uniform plug flow in the reactor, residence time (t) was estimated as $V(1 - \varepsilon)/Q$, where V ($W \times D \times L$) is the total volume of the reactor and Q is the volumetric flow rate.

The microreactor was placed on a uniform heating stage to control the experimental temperature with a variability of ±0.5 °C. To ensure temperature uniformity, temperature inside the microchannel was occasionally measured by inserting a thermocouple. A 2:1 mixture of toluene and ε-CL by volume was introduced into the microreactor at different flow rates, from 30 to 640 μL/min, corresponding to residence times of ≈240 to 15 s. For every data point, 3 mL of ε-CL and toluene mixture was passed through the reactor, if not specified otherwise. Similar to batch experiments, all the experiments were performed at least three times to determine the experimental variability.

Characterization. Gel permeation chromatography (GPC) was used to obtain molecular mass information. A Waters system equipped with a 1515 isocratic HPLC pump with online degassing, 717 Plus autosampler, 2414 refractive index detector, a guard column, and three mixed bed columns (HR0.5, HR3 and HR4E) with 5 μm particle size was used. The HR0.5, HR3, and HR4E columns are specified for molar mass separation range of 0−1000, 500−30 000, and 50−100 000) g/mol, respectively. Other GPC parameters were as follows: THF was the eluent at a flow rate of 0.35 mL/min, maintained at 30 °C, 5 mg/mL was the sample concentration and the injection volume was 40 μL. A series of narrow polydispersity polystyrene standards were used to calibrate the GPC system and the molecular masses reported here are relative to polystyrene standards. The uncertainty in the measurement of polystyrene equivalent molar mass is 10%.

Raman spectra for different samples were obtained using a Raman Systems (model R3000HR) Raman spectrometer. The instrument is

dx.doi.org/10.1021/ja111346c |J. Am. Chem. Soc. 2011, 133, 6006–6011

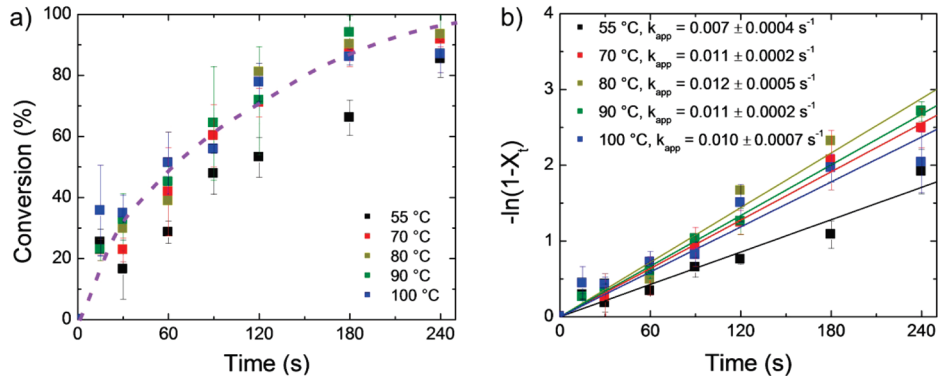

Figure 2. (a) Conversion of ε-caprolactone as a function of residence time for five temperatures. The dotted line is for visual guidance only, not a model fit. (b) Semilogarithmic plot of conversion data fitted with first-order reaction kinetics. The apparent rate constants are shown as inset. The errors indicate one standard uncertainty based on measurements on at least three different samples.

equipped with a laser having an excitation wavelength of 785 nm and a fiber optic probe. Spectra were collected for 60 s and data analysis was performed using GRAMS software.

RESULTS AND DISCUSSION

The ROP of ε-CL (Figure 1a) was performed in toluene at temperatures ranging from 55 to 100 °C. Because of their chemical resistance and excellent heat transfer properties, metal/silicon/ceramic microreactors[17] are preferred for these reactions compared to those made with polymers, such as polydimethylsiloxane (PDMS),[17,18] perfluoropolyethers,[19] and thiolene-based polymers.[14] For the present study, we chose aluminum microreactors (Figure 1b,c), which are inexpensive and easy to fabricate in contrast to silicon and ceramic reactors.[17] The channels were filled with 100 mg of N435 beads of diameter 400 ± 50 μm. A 2:1 mixture of toluene and ε-CL by volume was introduced in the microreactors at different flow rates, from 30 to 640 μL/min, corresponding to residence times, t, of ≈240−15 s.

The monomer conversion in microreactors was measured using Raman spectroscopy. With this technique, we captured the disappearance of the antisymmetric ring stretching peak of ε-CL at 696 cm^{-1}, as ε-Cl converted to PCL.[20] As indicated in the literature, activation of monomer by formation of the acyl−enzyme complex is the rate-limiting step.[6] This step involves opening of the ε-CL ring structure; therefore, disappearance of the ring structure, as captured by Raman spectroscopy, describes the apparent reaction rate. As displayed in Figure 2a, conversion increased with time. The experimental data was fitted with first-order reaction kinetics (Figure 2b) as follows:

$$-\ln(1 - X_t) = k_{app}t \qquad (1)$$

where, X_t is the fractional monomer conversion for a residence time of t and k_{app} is the apparent rate constant. Here, for simplicity, we have not normalized the rate constants with the effective catalyst amount, since it is difficult to determine the exact amount of available enzyme immobilized on porous beads.

The apparent rate of reaction was lowest at 55 °C and then increased to 70 °C; however, the reaction rate does not change significantly with further increase of temperature. Typically, reaction rate depends on two factors, catalytic (enzyme) and mass transfer rates. Reasonable first-order fitting of the data for all residence times indicate that mass transfer resistance for monomer is not significant for this system, at least at the lower residence times, where molecular mass of the products and viscosity are not high. Therefore, the chemical reaction step is the rate-limiting step. The nonmonotonic behavior of reaction rates observed here, which is much different than the Arrhenius behavior typically observed, is similar to previous reports on lactone ROP reactions[5,10] and esterifications of small molecules[21] in batch reactors. This nonmonotonic behavior of reaction rates at higher temperatures is likely due to the deactivation and denaturation of enzymes.[21]

We also compared the kinetics data of microreactors to that of batch reactors. As displayed in Figure 3, at 70 °C, the rate of reaction is much faster in the microreactor compared to the batch reactor. Over the tested temperature range, the apparent rate constants for the microreactors are in the range of 0.007 to 0.012 s^{-1}; whereas for the batch reactors, the rate constants vary from 0.0004 to 0.0008 s^{-1} (Supporting Information). Therefore, the apparent rate of reaction in microreactors is at least an order of magnitude higher than that observed for batch reactors. This can be attributed to two factors: (1) in the confined volume of microreactors, relative to batch reactors, reactants are forced to be in contact with enzyme active sites,[22] that is, transport path length in the microreactors is much smaller; and (2) as the surface-to-volume ratio in the microreactors is much higher than that of batch reactors, more enzyme active sites are available to reactants at any instance. A similar improvement in performance would be expected in batch reactors by increasing the amount of enzymes (to increase the surface-to-volume ratio). However, such an increase of the amount of enzymes immobilized on solid beads would be practically impossible due to difficulty of mixing at high solid contents and could cause breaking of particles and loss of enzymes from the solid bead surfaces due to mechanical shear. Furthermore, recovery of the enzyme would be impaired, dramatically increasing costs of the process.

The estimation of molecular mass for enzymatic ε-CL ROP reactions using gel permeation chromatography (GPC) poses a significant challenge. Unlike symmetrical, monomodal GPC traces typically reported for polyesters synthesized by chemical catalysts, we observed a long tail in addition to a broad polymer peak for all samples (inset Figure 4b and Supporting Information). This result is consistent with other reports on enzyme-catalyzed PCL synthesis.[23,24] Mass spectrometry results indicate that the tail consists of oligomeric compounds, both linear and cyclic,

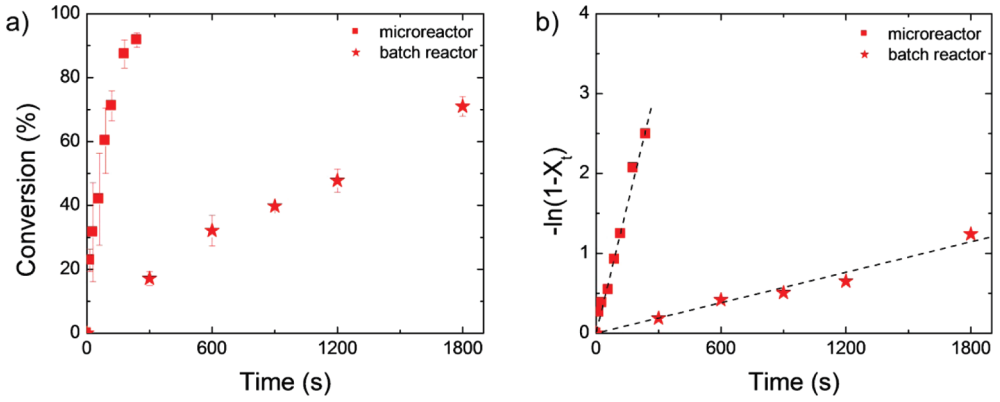

Figure 3. (a) Conversion as a function of time for batch and microreactors at 70 °C. (b) Conversion data fitted to first-order kinetics. The error bars indicate one standard uncertainty based on measurements on at least three different samples.

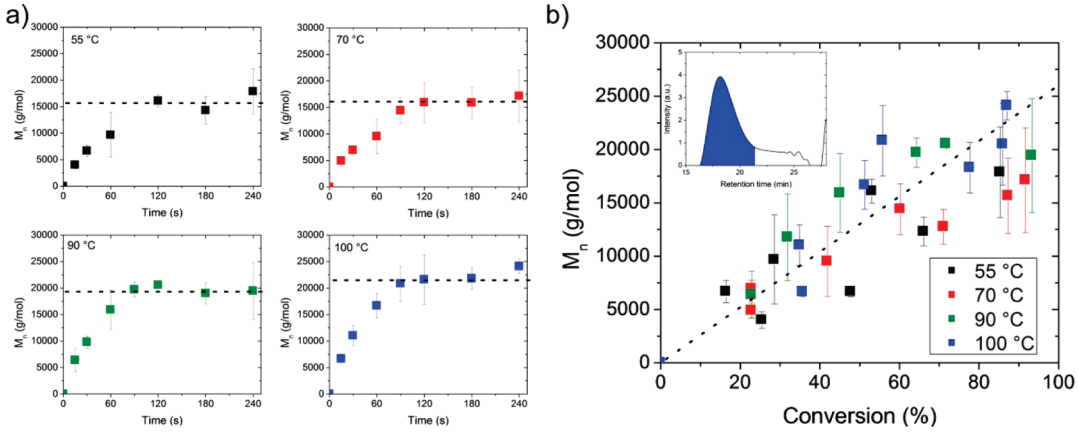

Figure 4. (a) Number average molecular mass (M_n) as a function of residence time at four temperatures. (b) M_n as a function of conversion. Inset shows GPC trace for a PCL sample. The error bars indicate one standard uncertainty based on measurements on at least three different samples.

however, mostly dominated by cyclic (see Supporting Information).[25,26] An estimated value of molar mass, particularly M_n (the number average relative molecular mass), depends on the selection of end point in the GPC trace, that is, the amount of low molecular mass species that are included in the estimation. To obtain self-consistent results for various experimental conditions presented here, we consistently used the inflection point of the broad polymer peak as the end point (inset Figure 4b and Supporting Information). Because of differences in our approach and those used in the literature to define polymer peaks, the molecular mass values reported here may differ from the literature. However, use of this analysis method enables valid data comparisons and the general trend in this data remains consistent with the literature.

The enzymatic polymerization reaction follows the 'activated monomer mechanism'.[6] In the initiation step, the acyl−enzyme complex formed during chain activation undergoes nucleophilic attack by bound water on the outer regions of the enzyme, resulting in formation of a ω-hydroxy-carboxylic acid, the shortest propagating component. In the subsequent chain propagation step, the terminal hydroxyl group of a propagating chain end performs nucleophilic attack on the acyl−enzyme complex to form a one-monomer unit longer oligomer/polymer chain.[6,8] The amount of available water determines the number of initiated chains, which further propagate to form longer chains. Similar to living polymerization, in principle, the monomer to water ratio determines the final molecular mass; however, initiation and chain propagation steps for this enzymatic polymerization reaction are not very efficient[8] and, as a result, not all initiated chains grow to larger chains. In addition to chain propagation, polycondenstation and intrachain transesterification reactions can also take place.[27] CAL B can also degrade PCL by chain scission;[24,28] however, the rate of degradation is slower than the rate of polymerization.[24] Molecular mass at any instance is determined by two competing reactions, polymerization and degradation.

Plots of M_n versus time for microreactors (Figure 4a) clearly show that M_n increases regularly with time up to about 120 s and then reach a plateau value indicating an equilibrium between the polymerization and the degradation reactions.[24,29] Plotting M_n as a function of conversion shows the same general trend at all experimental temperatures, M_n increases with conversion (Figure 4b). The observed increase in M_n with increased conversion is consistent with previous reports for batch enzyme-catalyzed ε-CL ROP reactions[5,27] and indicates propagation is by a chain growth mechanism, where monomer addition occurs at chain ends. The deviation from linearity of data in Figure 4b may be due to differences in low molecular mass content and fluctuations in nonideal flow condition in the microreactor as a function of flow rate (e.g., reaction time).

Furthermore, comparison of batch and microreactor systems herein (Figure 4a and Figure S6) show that, at identical reaction

dx.doi.org/10.1021/ja111346c |J. Am. Chem. Soc. 2011, 133, 6006–6011

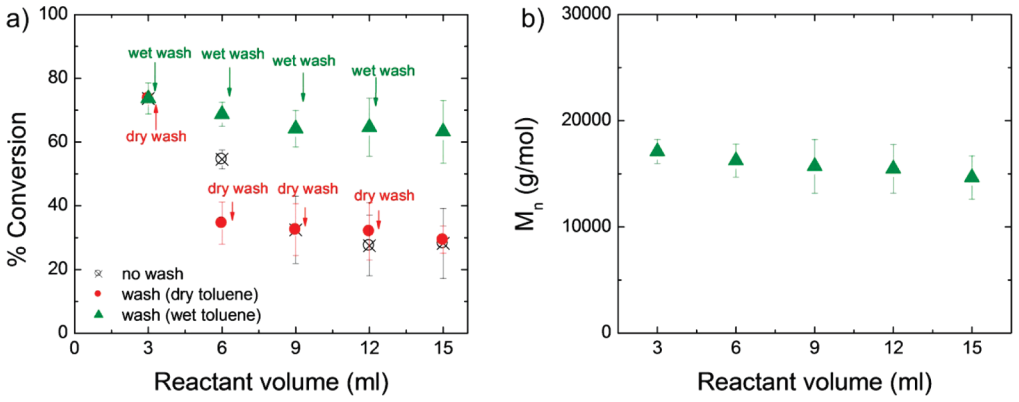

Figure 5. (a) Conversion as a function of reactant volume processed in the microreactor. "Dry wash" indicates that after every 3 mL of sample collection the microreactor was flushed with dry toluene, whereas in the "wet wash" case, flushing was performed with wet toluene. (b) M_n as a function of reactant volume for "wet wash". The experimental temperature was 70 °C and residence time in the microreactor was 120 s. The errors indicate one standard uncertainty based on measurements on at least three different samples.

temperatures, M_n reached higher values in microreactors. This is likely related to the diffusivity of polymer chains. Specifically, polymer chain ends must diffuse to enzyme active sites for chain propagation reactions to occur. As the viscosity of the system increases with polymerization, the diffusivity of chains decreases, thus, limiting chain propagation. However, the diffusion problem can be particularly important in batch reactors because of inefficient mixing; whereas in the confined space of microreactors, the diffusion path length is shorter and chain propagation to higher molecular mass can take place more easily. Diffusion improves with the increase of temperature as the diffusivity increases and the viscosity decreases, which may result in slightly higher molecular mass at higher temperatures in both batch and microreactors.

Reusability and extended service life are two important parameters which dictate the economic feasibility of enzymes in commercial applications. The present microreactor design enables us to study the change of enzyme efficiency during continuous flow synthesis over a prolonged period. In a set of experiments, we processed 15 mL of reactants through the microreactors at a fixed residence time and collected 5 samples with 3 mL volume each to determine the stability of conversion and molecular mass during a prolonged run. If no treatment was performed in between collection steps (no wash), the conversion decreased significantly with the continuous processing of reactants (Figure 5). To determine whether the decrease of conversion was caused by adsorption and accumulation of PCL on CAL B-loaded beads, we flushed the microreactors with dry toluene after every 3 mL of sample collection (dry wash). This had little effect on the results, ruling out the possibility of polymer deposition. It is likely that, during the continuous flow process, most of the water was consumed, which resulted in lower monomer conversion. Also, the lower water concentration reduced CAL B activity. Decrease in enzyme activity at lower water concentration is generally explained in the literature as water acting as a lubricant for enzymes, and therefore, as water is removed from enzymes, they become stiffer and less active.[30] To test the hypothesis that water depletion was the cause of the decrease of conversion, we flushed the microreactor with toluene saturated with water after every 3 mL of sample collection (wet wash). During the washing process, enzymes absorbed water from toluene and regained their activity, which resulted in nearly constant conversion and M_n (Figure 5, panels a and b, respectively). This strategy will be important for enzyme-catalyzed chemical synthesis, where water content depletes continuously due to its involvement in the synthesis.

Although we addressed several important issues, another critical parameter for enzyme-catalyzed reactions is leaching of enzymes from solid beads into products. Such leaching contaminates products while also reducing biocatalyst (immobilized enzyme) service lifetime. A preliminary study by us indicates that enzyme leaching is lower in microreactors compared to the batch reactors; however, the quantification of enzyme present in the products (less than 1%) poses a significant measurement challenge. Further research into a robust quantitative method is ongoing.

CONCLUSION

In this paper, we have reported the application of a microreactor based platform for studying enzymatic polymerization reactions in continuous flow mode. The versatile reactor design enabled us to change the reaction conditions readily and to achieve faster product formation compared to conventional batch reactors. While this study focused on enzyme-catalyzed lactone polymerization reactions, it is evident that similar microreactor based platforms can readily be extended to other systems, for example, high-throughput screening of new enzymes and to processes where continuous flow mode is preferred.

ASSOCIATED CONTENT

Supporting Information. Estimation of conversion from Raman spectra, estimation of molecular mass from GPC traces, MALDI-MS results, and results from batch experiments. This material is available free of charge via the Internet at http://pubs.acs.org.

AUTHOR INFORMATION

Corresponding Author

*rgross@poly.edu; beers@nist.gov

Author Contributions

#These authors contributed equally.

■ ACKNOWLEDGMENT

A.S.B. and R.A.G. would like to acknowledge the NSF center for Biocatalysis and Bioprocessing at NYU-POLY for its financial support.

■ REFERENCES

(1) US Department of Energy, Office of Energy Efficiency and Renewable Energy, Office of the Biomass Program, Washington, DC, 2003.

(2) Wolf, O.; Crank, M.; Patel, M.; Marscheider-Weidemann, F.; Schleich, J.; Hüsing, B.; Angerer, G. *Techno-Economic Feasibility of Large-Scale Production of Bio-Based Polymers in Europe*; EUR 22103 EN; European Communities: Spain, 2005.

(3) Committee on Grand Challenges for Sustainability in the Chemical Industry; National Research Council. *Sustainability in the Chemical Industry: Grand Challenges and Research Needs—A Workshop Report*; National Academies Press: Washington, DC, 2005.

(4) Drauz, K.; Waldmann, H. *Enzyme Catalysis in Organic Synthesis: A Comprehensive Handbook*; Wiley-VCH: New York1995.

(5) Gross, R. A.; Kumar, A.; Kalra, B. *Chem. Rev.* **2001**, *101*, 2097.

(6) Kobayashi, S. *Macromol. Rapid Commun.* **2009**, *30*, 237.

(7) Labet, M.; Thielemans, W. *Chem. Soc. Rev.* **2009**, *38*, 3484.

(8) Duda, A.; Kowalski, A.; Penczek, S.; Uyama, H.; Kobayashi, S. *Macromolecules* **2002**, *35*, 4266.

(9) Truhlar, D. G.; Kohen, A. *Proc. Natl. Acad. Sci. U.S.A.* **2001**, *98*, 848.

(10) Mei, Y.; Kumar, A.; Gross, R. A. *Macromolecules* **2002**, *35*, 5444.

(11) Sanjay, G.; Sugunan, S. *Catal. Commun.* **2005**, *6*, 81.

(12) Hogan, J. *Nature* **2006**, *442*, 351.

(13) Wilms, D.; Klos, J.; Frey, H. *Macromol. Chem. Phys.* **2008**, *209*, 343.

(14) Wu, T.; Mei, Y.; Cabral, J. T.; Xu, C.; Beers, K. L. *J. Am. Chem. Soc.* **2004**, *126*, 9880.

(15) Iida, K.; Chastek, T. Q.; Beers, K. L.; Cavicchi, K. A.; Chun, J.; Fasolka, M. J. *Lab Chip* **2009**, *9*, 339.

(16) Miyazaki, M.; Maeda, H. 2006, *24*, 463.

(17) Hartman, R. L.; Jensen, K. F. *Lab Chip* **2009**, *9*, 2495.

(18) Whitesides, G. M. *Nature* **2006**, *442*, 368.

(19) Rolland, J. P.; Van Dam, R. M.; Schorzman, D. A.; Quake, S. R.; DeSimone, J. M. *J. Am. Chem. Soc.* **2004**, *126*, 2322.

(20) Colwell, J. M.Doctoral Dissertation, Queensland University of Technology, 2006.

(21) Pirozzi, D.; Greco, G. *Enzyme Microb. Technol.* **2004**, *34*, 94.

(22) Losey, M. W.; Schmidt, M. A.; Jensen, K. F. *Ind. Eng. Chem. Res.* **2001**, *40*, 2555.

(23) Thurecht, K. J.; Heise, A.; deGeus, M.; Villarroya, S.; Zhou, J.; Wyatt, M. F.; Howdle, S. M. *Macromolecules* **2006**, *39*, 7967.

(24) Sivalingam, G.; Madras, G. *Biomacromolecules* **2004**, *5*, 603.

(25) Bankova, M.; Kumar, A.; Impallomeni, G.; Ballistreri, A.; Gross, R. A. *Macromolecules* **2002**, *35*, 6858.

(26) Córdova, A.; Iversen, T.; Hult, K.; Martinelle, M. *Polymer* **1998**, *39*, 6519.

(27) Mei, Y.; Kumar, A.; Gross, R. *Macromolecules* **2003**, *36*, 5530.

(28) Kobayashi, S.; Uyama, H.; Takamoto, T. *Biomacromolecules* **2000**, *1*, 3.

(29) Kobayashi, S.; Takeya, K.; Suda, S.; Uyama, H. *Macromol. Chem. Phys.* **1998**, *199*, 1729.

(30) Dong, H.; Cao, S.-G.; Li, Z.-Q.; Han, S.-P.; You, D.-L.; Shen, J.-C. *J. Polym. Sci., Part A: Polym. Chem.* **1999**, *37*, 1265.

CONTINUOUS FLOW ENZYME-CATALYZED POLYMERIZATION IN A MICROREACTOR

Santanu Kundu,[1†] Atul S. Bhangale,[2†] William E. Wallace,[1] Kathleen M. Flynn,[1] Charles M. Guttman,[1] Richard A. Gross,[2] and Kathryn L. Beers[1*]*

Supporting Information

Estimation of conversion from Raman spectra

Upon ring opening of ε-caprolactone (ε-CL), the anti-symmetric ring stretching peak at 696 cm^{-1} disappears. Therefore, monitoring the change in intensity of this peak as the reaction progresses allows estimation of percentage monomer conversion. To obtain quantitative information from Raman spectroscopy on monomer conversion a calibration curve was generated from pure compounds. Hence, two stock solutions of PCL and ε-CL in toluene with a concentration of 0.4 g/mL were prepared. These solutions were mixed in various ratios to change the ratio of ε-CL-to-PCL while maintaining the same total concentration of these mixture components. The solution, where the ratio of ε-CL-to-PCL is 3:1, mimics polymerization reactions with 25 % conversion of ε-CL to PCL. Similarly, different monomer conversions were simulated by changing the ratio of ε-CL-to-PCL in the solution. Raman spectra for different ratios of ε-CL-to-PCL are shown in **Figure S1a**. The peak at 1003 cm^{-1}, corresponding to ring breathing of toluene, is considered as an internal standard, since there is no spectral contribution from ε-CL at this wave number. The peak at 696 cm^{-1} decreases as the concentration of ε-CL decreases and by determining the ratio of peak areas at 696 cm^{-1} to that at 1003 cm^{-1} (after deconvolution of the spectra) for different ε-CL concentrations, a calibration plot was generated (**Figure S1b**). This calibration plot was used to determine ε-CL conversion during polymerization reactions.

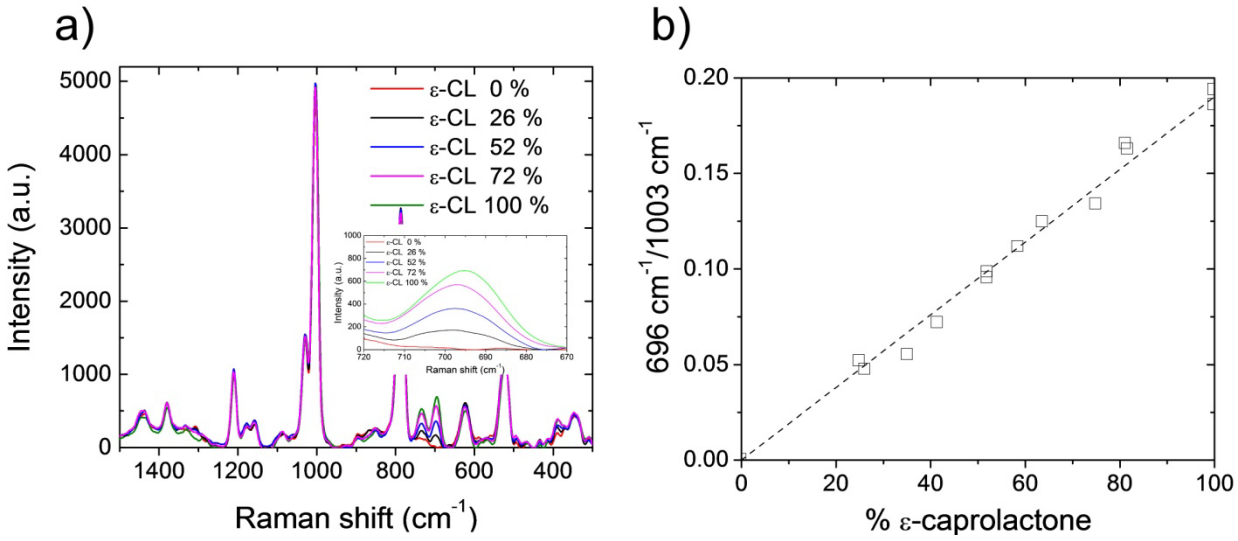

Figure S1: (a) Raman spectra for different ratios of ε-caprolactone and poly(ε-caprolactone). All spectra have been baseline corrected. Inset shows peak intensities at 670 to 720 cm^{-1}. (b) calibration curve to determine ε-caprolactone concentration by determining the ratio of peak areas at 696 cm^{-1} to that at 1003 cm^{-1}. Dashed line indicates the calibration curve.

Estimated monomer conversion values by Raman spectroscopy were compared to those determined by Nuclear Magnetic Resonance (NMR). Results displayed in **Figure S2** show that there is excellent agreement between monomer conversion values determined by NMR and Raman spectroscopy.

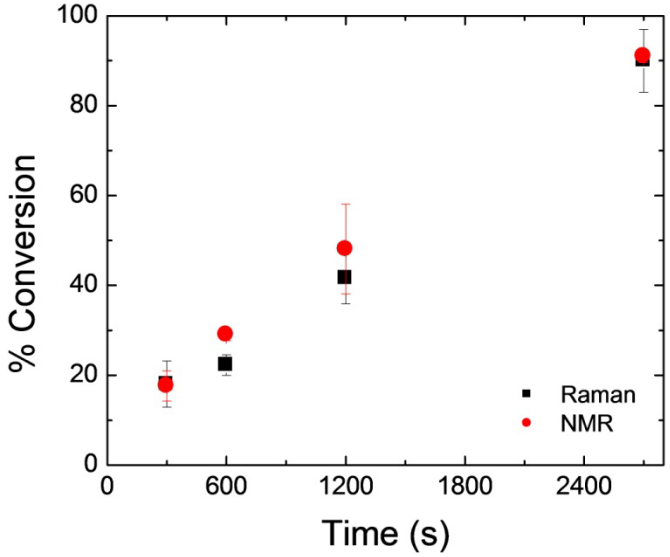

Figure S2: Conversion as a function of time determined by ^{1}H NMR and Raman spectroscopy. The error bars indicate one standard uncertainty based on measurements on at least three different samples.

Estimation of molecular mass:

Figure S3 displays a typical GPC trace of a sample obtained from a microreactor with ε-CL conversion to PCL of 50 %. GPC traces for ε-CL ROP using N435 as catalyst typically display a long tail after a broad peak. The broad peak is associated with PCL of higher molecular mass whereas, the long tail represents lower molecular mass oligomeric compounds. The later was verified by MALDI-MS analysis (see below), which also showed cyclic compounds are most abundant in the low oligomeric tail, consistent with previous studies. Since the polymer peak in the GPC trace is not symmetrical, the estimated molecular mass will depend on the amount of low molecular mass species that are included in the calculation. As shown in **Figure S3a**, if we consider the blue region, the estimated M_n and PDI values are 13,000 and 2.3, respectively. However, if more low molecular mass compounds are included in the calculation, as shown in **Figure S3b**, M_n and PDI values change to 7,300 and 3.7, respectively. For **Figure S3a**, the inflection point of the broad polymer peak is selected as the end point. This identical protocol was used to estimate molecular mass for all samples analyzed herein.

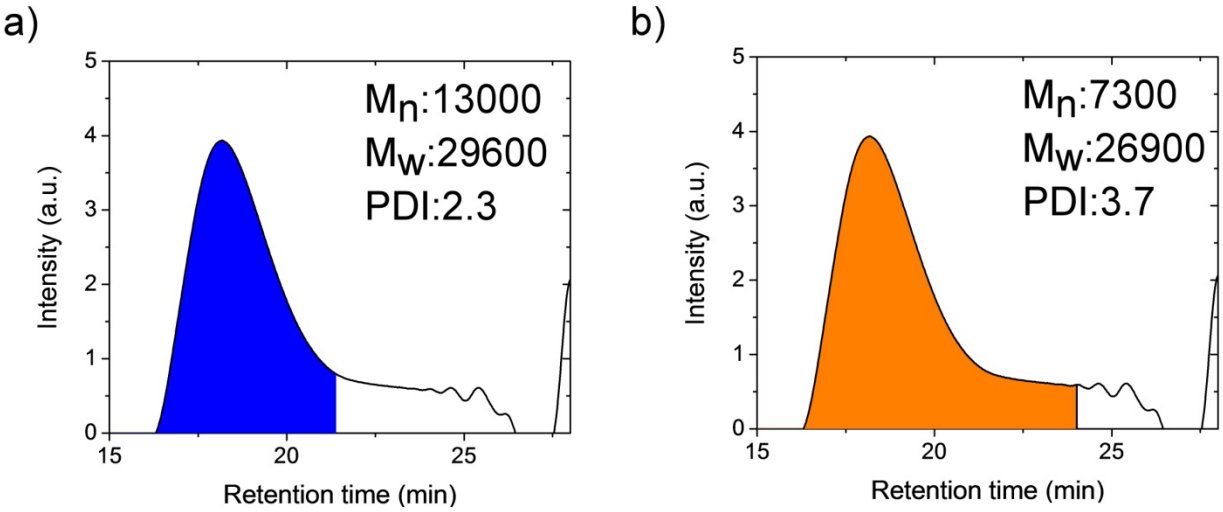

Figure S3: Typical GPC trace of a sample. The colored regions represent portions of the GPC trace that were included in calculations to determine PCL molecular mass averages and PDI values.

MALDI-MS results:

The mass spectrometry was performed on a Bruker REFLEX II time-of-flight instrument in reflection mode using delayed ion extraction. Ions were generated using a nitrogen gas laser with an average energy of approximately 5 microJoules per pulse spread over a spot size 100 μm in diameter. The dithranol MALDI matrix was dissolved in acetone at a concentration of approximately 20 mg/mL. The

polycaprolactone analyte, which came as a concentrated solution in toluene, was diluted with toluene to a concentration of approximately 1 mg/mL. The two solutions were mixed in a ratio of 5 to 1 and the sample was hand spotted from the mixed solution. The ratio of matrix to analyte was on the order of 100 to 1 by mass. The uncertainty in ion mass was 0.1 u and in intensity from spectrum to spectrum was about 15%.

The results for a typical sample are shown in **Figure S4**. The dominance of cyclic oligomers below a degree of polymerization of 10 was typical both for batch and microfluidic samples. Fractionation studies showed that these low mass cyclic oligomers correspond to the long elution time ringing in the gel permeation chromatograms.

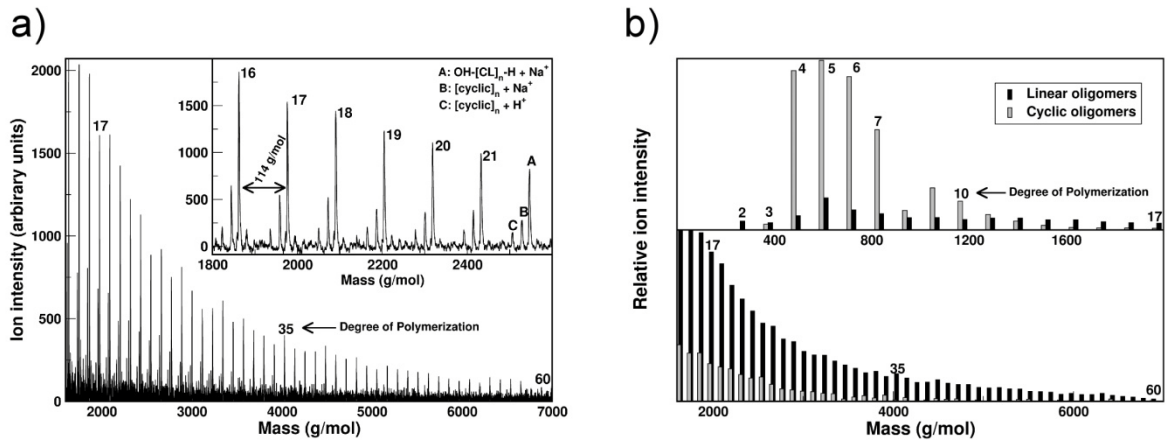

Figure S4: (a) Mass spectrum of a PCL sample showing oligomers up to 7000 g/mol in mass (degree of polymerization of 60). The figure inset shows the 114 g/mol repeat spacing and the three characteristic peaks, one linear and two cyclic, found at each degree of polymerization. (b) Reduced mass spectral data where the intensities for the two cyclic peaks in mass spectrum were summed and are shown as a single peak. The dominance of cyclic oligomers below a degree of polymerization of 10 was typical both for batch and microfluidic samples.

Batch experiments:

We also performed N435 catalyzed ε-CL ROP reactions in batch reactors at temperatures ranging from 55 °C to 100 °C. Monomer conversion as a function of time is displayed in **Figure S5a** and the semi-logarithmic plot in **Figure S5b** indicates that the polymerization reaction follows first order kinetics. Similar to microreactors, the rate of the reaction was lowest at 55 °C and then increases slightly at the higher temperatures studied. Furthermore, similar to microreactor experiments, differences in values obtained for apparent rate constants at higher temperatures (e.g. 70 °C to 100 °C) are not significant.

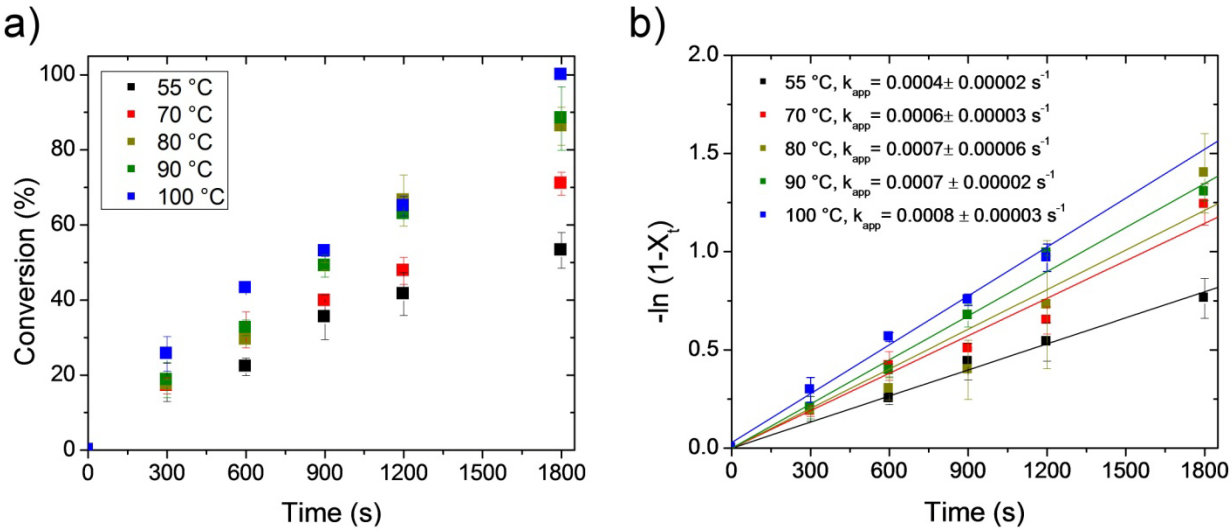

Figure S5: (a) Monomer conversion as a function of reaction time at five different temperatures. (b) Conversion data fitted to first order kinetics. The error bars indicate one standard uncertainty based on measurements on at least three different samples.

Measurements by GPC of PCL M_n values as a function of reaction temperature and time are displayed in **Figure S6**. Observation of **Figure S6** shows that M_n increases regularly with time and no plateau regions were observed. However, maximum PCL M_n values reached in batch reactor studies were lower than those obtained from N435 catalyzed ε-CL ROP performed in microreactors.

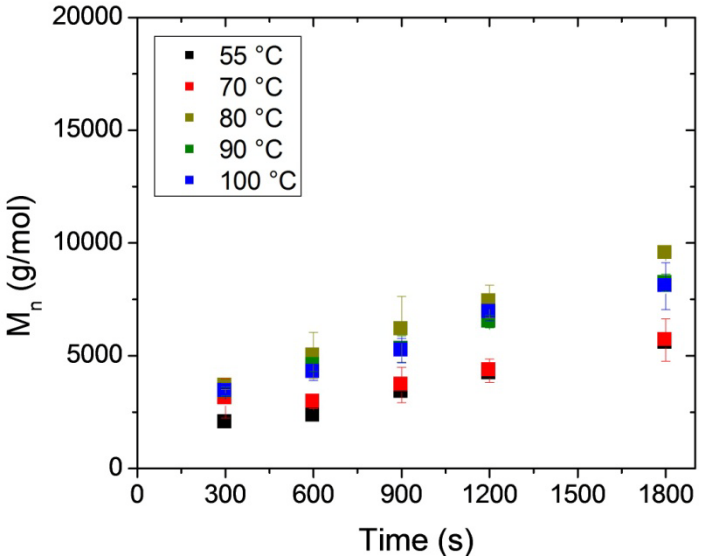

Figure S6: M_n as a function of reaction time for polymerizations conducted at different temperatures. The error bars indicate one standard uncertainty based on measurements on at least three different samples.

Plotting M_n as a function of conversion for batch N435 catalyzed ε-CL ROP reactions shows the general trend of that at 55 °C to 100 °C, M_n increases with conversion (**Figure S7**). This indicates that propagation is by a chain polymerization mechanism where monomer addition occurs from chain ends.

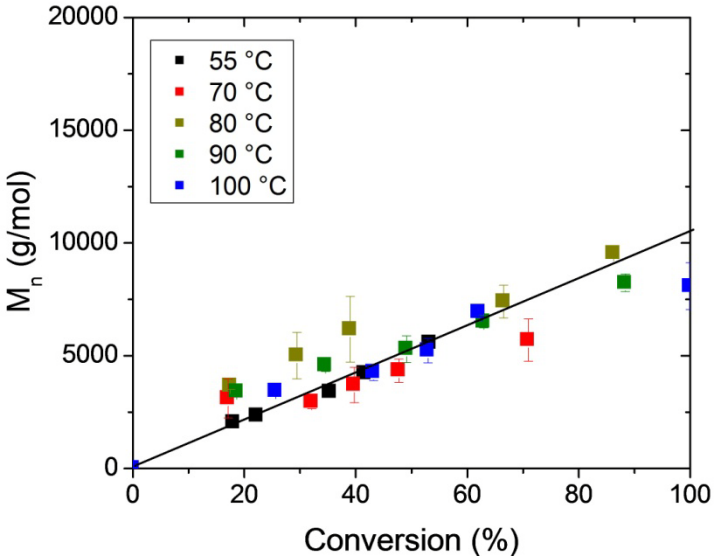

Figure S7: M_n as a function of ε-CL conversion for N435 catalyzed polymerizations conducted in batch reactors. The line in the graph is to guide the eye and does not represent a mathematical fit to the data. The error bars indicate one standard uncertainty based on measurements on at least three different samples.

GPC traces of the samples collected during continuous runs are shown in Figure S8. For wet wash, where the conversion was similar after every wash, the GPC traces remained similar including the low molecular mass tail indicating similar molecular mass distribution. Whereas, for dry wash as the conversion decreased, the GPC traces also changed. Particularly, the ratio between the intensity of high molecular mass peak and to that of low molecular mass tail decreased indicating presence of more oligomeric compounds.

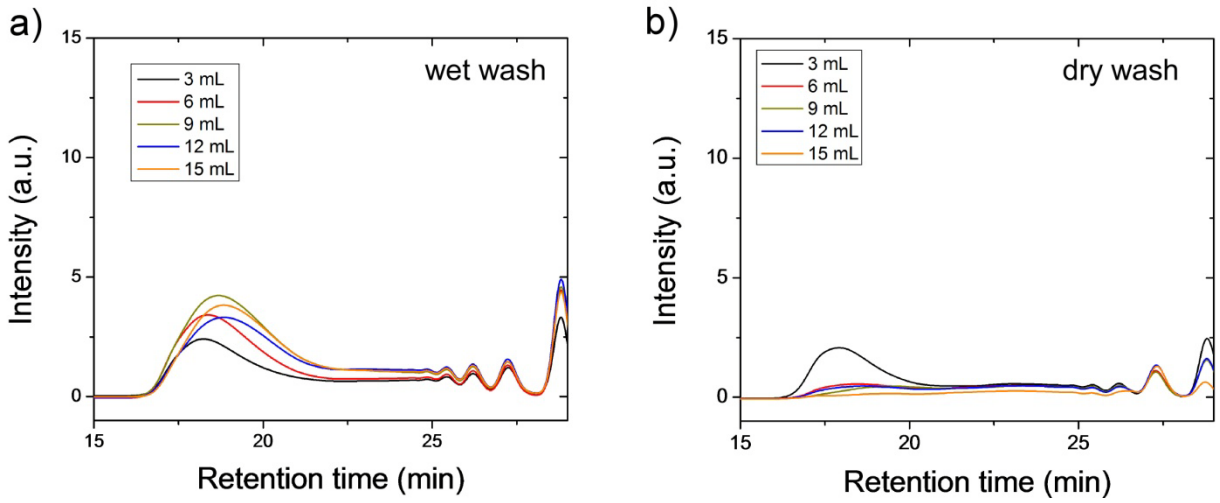

Figure S8: GPC traces of the samples collected during the (a) wet wash and (b) dry wash.